Electronic Supplementary Material (ESI) for Journal of Materials Chemistry B.

Supplementary Information

Molecular Co-assembling of Multicomponent Peptides for Generation of Nanomaterials with Improved Peroxidase Activities

Yehao Zhang,[a] and Xinming Li *[a,b]

[a.] College of Chemistry, Chemical Engineering and Materials Science, Soochow University, Suzhou, 215123, China.
[b.] Jiangsu Engineering Laboratory of Novel Functional Polymeric Materials, Soochow University, Suzhou, 215123, China

Contents

1. Materials and methods

2-chlorotrityl chloride resin, *O*-benzotriazol-1-yl-tetramethyluronium hexafluorophosphate (HBTU), Fmoc-Val-OH, Fmoc-His(Trt)-OH, Fmoc-Asn(Trt)-OH, Fmoc-Gln(Trt)-OH, Fmoc-Arg(Pbf)-OH, Fmoc-Lys(Boc)-OH, Fmoc-Asp(OtBu)-OH, Fmoc-Ser(OtBu)-OH, Fmoc-Phe-OH, Fmoc-Glu(OtBu)-OH,and, Fmoc-Gly-OH, Fmoc-Tyr(tBu)-OH were purchased from GL Biochem (Shanghai, China). 2-(naphthalen-6-yl) acetic acid was provided by Aladdin (Shanghai, China). Piperidine, trifluoroacetic acid (TFA) and *N,N*-diisopropylethylamine (DIEA) were provided by Energy Chemical and Adamas, respectively. Phosphate buffered solution (10 mM) was obtained from Sangong Bioengineering (Shanghai, China). Superoxide dismutase was supplied by Shanghai Yuanye Biotechnology. 3,3',5,5'-tetramethylbenzidine (TMB) was provided by Macklin and tertiary butanol were purchased from Aladdin. Hemin was purchased from Bide Pharmatech Co. ^{1}H NMR spectra were recorded on the Unity Inova 400 MHz by using DMSO-*d6* as the solvent. MALDI-TOF mass spectrometry analysis was conducted on the Bruker Ultraflex-Treme mass spectrometer (Germany). Circular dichroism spectra (CD) were collected from the JASCO J-810 spectrometer (Japan). Fourier transform infrared spectroscopy (FTIR) characterizations were carried out on the PerkinElmer spectrophotometer (USA). Transmission electron micrograph (TEM) images were recorded on the Hitachi HT7700 TEM. UV-Vis spectroscopy analysis was performed on the UV-1900i (Shimadzu (Suzhou) Instrument Co. LTD, China). Fluorescence spectra were obtained from F-2700 fluorescence spectrophotometer (Japan) and BioTek Synergy Neo microplate reader. High Performance Liquid Chromatography (HPLC) analysis were conducted on a Waters 2489 with a UV/Visible Detector by using CH_3CN (0.1% of TFA) and H_2O (0.1% of TFA) as eluents.

2. Experimental section

2.1 Peptide Synthesis:

The peptides were synthesized from corresponding amino acids based on the solid-phase peptide synthesis (SPPS) technique with the 2-chlorotrityl chloride resin (100-200 mesh and 1.3-1.8 mmol/g). First, 0.5 g resin was swelled in dry dichloromethane

(DCM) with N_2 for 30 min and the swelled resin was washed by dry *N, N*-dimethylformamide (DMF) for five times. Then the DMF solution containing N,N-diisopropylethylamine (DIEA) and Fmoc-His(Trt)-OH was added to react for 1.5 h and the resin was washed with dry DMF for four times. Afterward, the blocking solution (16:3:1 of DCM / MeOH / DIEA) was added to quench the resin for 10 min, and the resin was rinsed thoroughly with dry DMF. Then the resin was treated with 20 % piperidine (in DMF) for 0.5 h to remove Fmoc-protecting groups and washed with DMF for four times. The designed molecule was elongated step by step by following standard Fmoc solid phase peptide synthesis protocols, and HBTU was used as a coupling reagent. Ultimately, the synthetic peptide was cleaved from the resin by using cleavage solution (TFA: H_2O = 95:5). The final yields of synthetic peptides were about 80 %.

NapFFKH: ^{1}H NMR (400 MHz, DMSO-d_6) δ 8.86 (s, 1H), 8.23 (ddd, J = 87.3, 30.0, 8.0 Hz, 4H), 7.89 – 7.82 (m, 1H), 7.79 – 7.69 (m, 4H), 7.58 (d, J = 1.6 Hz, 1H), 7.47 (tt, J = 6.9, 5.1 Hz, 2H), 7.36 – 7.32 (m, 1H), 7.24 – 7.12 (m, 10H), 4.61 – 4.46 (m, 3H), 4.25 (td, J = 8.3, 5.4 Hz, 1H), 3.58 (d, J = 14.1 Hz, 1H), 3.50 (s, 1H), 3.16 (dd, J = 15.3, 5.4 Hz, 1H), 3.06 – 2.88 (m, 3H), 2.83 – 2.66 (m, 4H), 1.69 – 1.60 (m, 1H), 1.52 (p, J = 8.1, 7.7 Hz, 3H), 1.31 (d, J = 8.7 Hz, 2H). MS: calcd M =745.3588, obsd $(M + H)^+$= 746.9466, obsd $(M + Na)^+$ =768.8512, obsd $(M + K)^+$=784.7721.

NapFFQH: ^{1}H NMR (300 MHz, DMSO-d6) δ 8.96 (s, 1H), 8.36 (dd, J = 19.6, 8.3 Hz, 2H), 8.21 (d, J = 7.5 Hz, 1H), 8.12 (d, J = 8.0 Hz, 1H), 7.85 (d, J = 7.5 Hz, 1H), 7.75 (t, J = 9.1 Hz, 2H), 7.57 (s, 1H), 7.54 – 7.35 (m, 4H), 7.27 – 7.13 (m, 11H), 6.82 (s, 1H), 4.54 (d, J = 17.4 Hz, 3H), 4.24 (d, J = 6.6 Hz, 1H), 3.60 (s, 1H), 3.17 (dd, J = 15.4, 5.3 Hz, 1H), 2.99 (td, J = 14.8, 6.1 Hz, 3H), 2.75 (dt, J = 23.5, 11.6 Hz, 2H), 2.11 (d, J = 8.3 Hz, 2H), 1.90 (s, 1H), 1.77 (d, J = 10.8 Hz, 1H). MS: calcd M = 745.3224, obsd $(M + H)^+$= 746.4902, obsd $(M + Na)^+$ = 768.4788, obsd $(M + K)^+$=784.4547.

NapFFNH: ^{1}H NMR (300 MHz, DMSO-d_6) δ 8.96 (s, 1H), 8.25 (ddd, J = 41.4, 21.2, 7.7 Hz, 4H), 7.90 – 7.69 (m, 3H), 7.57 (s, 1H), 7.49 – 7.36 (m, 4H), 7.26 – 7.09 (m, 11H), 6.98 (d, J = 18.7 Hz, 1H), 4.54 (q, J = 8.0, 7.2 Hz, 4H), 3.60 (s, 1H), 3.55 (s,

1H), 3.49 (s, 1H), 3.17 (dd, *J* = 15.3, 4.8 Hz, 1H), 3.00 (ddd, *J* = 23.2, 14.2, 4.1 Hz, 3H), 2.73 (td, *J* = 14.0, 10.0 Hz, 2H). MS: calcd M = 731.3067 obsd $(M + H)^+$= 732.4942, obsd $(M + Na)^+$ = 754.4803, obsd $(M + K)^+$=770.4875.

NapFFNHNH: ^{1}H NMR (400 MHz, DMSO-d_6) δ 8.65 (d, *J* = 16.5 Hz, 2H), 8.44 – 8.26 (m, 4H), 8.16 (dd, *J* = 8.1, 3.8 Hz, 2H), 7.89 – 7.81 (m, 1H), 7.79 – 7.70 (m, 2H), 7.57 (s, 1H), 7.47 (tt, *J* = 7.2, 5.3 Hz, 2H), 7.36 (s, 1H), 7.33 – 7.09 (m, 14H), 7.06 (s, 1H), 6.95 (s, 1H), 4.54 (ddtd, *J* = 21.4, 13.4, 8.4, 4.7 Hz, 6H), 3.58 (d, *J* = 14.1 Hz, 1H), 3.48 (d, *J* = 14.1 Hz, 1H), 3.12 (dd, *J* = 15.2, 5.0 Hz, 2H), 3.05 – 2.88 (m, 4H), 2.85 – 2.64 (m, 3H), 2.62 – 2.52 (m, 3H). MS: calcd M = 982.4086, obsd $(M + H)^+$= 983.6697, obsd $(M + Na)^+$ = 1005.6590.

NapFFNHNHNH: ^{1}H NMR (400 MHz, DMSO-d_6) δ 8.94 (d, *J* = 13.9 Hz, 3H), 8.48 – 8.10 (m, 8H), 7.88 – 7.81 (m, 1H), 7.78 – 7.71 (m, 2H), 7.59 (d, *J* = 15.1 Hz, 2H), 7.46 (dddd, *J* = 8.7, 6.8, 4.9, 2.2 Hz, 3H), 7.39 (d, *J* = 5.6 Hz, 1H), 7.32 (d, *J* = 4.8 Hz, 1H), 7.22 – 7.12 (m, 11H), 7.08 (s, 1H), 7.04 (s, 1H), 6.99 (s, 1H), 4.52 (h, *J* = 7.1, 6.4 Hz, 8H), 3.60 (s, 1H), 3.56 (s, 1H), 3.49 (s, 1H), 3.46 (s, 1H), 3.15 (dd, *J* = 15.9, 5.9 Hz, 3H), 3.05 – 2.90 (m, 6H), 2.78 – 2.65 (m, 2H), 2.62 – 2.53 (m, 3H). MS: calcd M = 1233.5104, obsd $(M + H)^+$= 1234.7226, obsd $(M + Na)^+$=1256.7174, obsd $(M + K)^+$=1278.6968.

NapFFHEKRH:1H NMR (400 MHz, DMSO-d6) δ 8.95 (s, 2H), 8.40 – 8.30 (m, 3H), 8.23 (d, J = 7.7 Hz, 1H), 8.10 (d, J = 7.5 Hz, 1H), 7.97 (d, J = 7.9 Hz, 1H), 7.84 (dd, J = 7.1, 2.3 Hz, 1H), 7.78 – 7.70 (m, 4H), 7.66 – 7.61 (m, 1H), 7.57 (d, J = 1.5 Hz, 1H), 7.50 – 7.42 (m, 2H), 7.38 (d, J = 1.3 Hz, 1H), 7.32 (d, J = 1.3 Hz, 1H), 7.24 – 7.13 (m, 10H), 4.65 (q, J = 7.4 Hz, 1H), 4.52 (dt, J = 14.2, 8.3 Hz, 3H), 4.29 – 4.15 (m, 3H), 3.60 (s, 1H), 3.56 (s, 1H), 3.16 – 2.88 (m, 8H), 2.82 (dd, J = 14.1, 9.5 Hz, 1H), 2.71 (d, J = 14.0 Hz, 3H), 2.34 – 2.16 (m, 2H), 2.00 (dd, J = 14.7, 7.0 Hz, 2H), 1.82 (d, J = 8.3 Hz, 1H), 1.56 (d, J = 65.1 Hz, 7H). MS: calcd M = 1167.5614, obsd $(M +H)^+$ = 1168.8712

2.2 TEM Characterizations

Each sample (4 μL) was placed on a carbon-coated copper grid and then stained with phosphotungstic acid (2.0 % w/v) for 10-15 min. The nanostructures within

sample were observed by the transmission electron microscope (Hitachi HT7700).

2.3 CD and FTIR Characterizations

CD spectra were recorded on a Jasco J-810 spectrometer. 25 μL of sample were loaded into a 1 mm thick quartz cell and scanned from 190 nm to 600 nm under N_2 atmosphere. FTIR spectra were collected with a PerkinElmer spectrophotometer. The sample was loaded into a KBr cuvette using deuterium oxide (D_2O) as a solvent. All spectra were scanned 64 times over the range of 3500-900 cm^{-1}.

2.4 Rheological Tests

The rheological tests were performed using a Thermo Scientific HAAKE RheoStress 6000 rheometer. 200 μL of hydrogel was placed on a 20 mm parallel plate for dynamic strain scanning tests. (i) Strain was increased from 0.01 to 10% at 6.28 rad/s and 25°C. (ii) Dynamic frequency scan tests were run at 1.0% from 0.1 to 10 Hz to ensure linear viscoelasticity.

2.5 Determination of the critical self-assembling concentration of peptides

A series of peptides solutions with the concentration from 0 to 4000 μg/mL were prepared in PBS buffer. After incubating with Thioflavin T (20 μM) for 12 h in dark, the fluorescence intensities of the peptide solutions containing Thioflavin T were measured on a F-2700 fluorescence spectrophotometer at 25 ℃ (λ_{ex} = 440 nm, λ_{em} = 490 nm). The critical self-assembling concentration of peptides was obtained according to the dose-dependent curve plotted with fluorescence intensities of Thioflavin T versus varied concentrations of peptides.

2.6 Co-assembly of peptides and Hemin

Hemin stock solutions were prepared in DMSO with a final concentration at 12.5 mM. Peptides were dissolved in ultrapure water followed by adjustment of pH to 7.4, and then mixed with the hemin solution. The mixture was subject to sonication together with pH adjustment to produce a uniformly dispersed solution. Ultimately, the solutions were heated in water bath to 90℃ and incubated at room temperature for 12h. The final concentrations of the peptide and hemin were 2.5 mM and 0.25 mM, respectively (peptide: hemin=10:1).

2.7 Determination of the peroxidase-like catalytic activity

The peroxidase-like catalytic activity was determined by adding 10 μL of TMB solution (4×10^{-2} M in acetonitrile solution) and 20 μL of H_2O_2 (0.15 M) into 930 μL of PBS buffer (1×10^{-2} M, pH 7.4). The mixture was homogenized by vortexing and then was incubated under 25 ℃ in a 10 mm path length quartz cuvette. The reaction was initiated by adding 40 μL of the peptide-hemin complexes (2.5×10^{-3}M). The oxidized product of TMB (oxTMB) was quantified by monitoring the absorbance at 640 nm using a UV-vis spectrophotometer (UV-1900i).

2.8 The effect of the pH and molar ratio between peptide and hemin on the catalytic activity

The pH of the solution was pre-adjusted within the range of 4.0–8.0, and the reaction was performed at 25 °C (peptide 2.5×10^{-3}M, peptide: hemin=10:1). The concentration of hemin was fixed at 0.25 mM, and the concentration of peptide was changed to prepare different ratios of peptide-heme complexes. The reactions were conducted at 25 °C, pH = 7.4. The initial reaction rate (v_0) for oxTMB production was determined to represent the catalytic activity of the peroxidase mimics.

2.9 Determination of reactive oxygen species involved in the process of TMB oxidation

The reactive oxygen species were determined by adding 10 μL of SOD (1×10^{-2} M in PBS buffer) or 20 μL of TBA (1×10^{-2} M in ultrapure water) to the catalytic system, which contained 10 μL of TMB solution (4×10^{-2} M in acetonitrile solution), and 20 μL of H_2O_2 (0.15 M in ultrapure water) in 966 μL of ×PBS buffer (10mM, pH 7.4). The mixture was homogenized by vortexing and then was incubated under 25 ℃ in a 10 mm path length quartz cuvette. The reaction was initiated by adding 4 μL of peptide-hemin complexes (2.5×10^{-3}M peptide: hemin=10:1). The production of oxidized TMB (oxTMB) was quantified by monitoring the absorbance at 640 nm using a UV-vis spectrophotometer (UV-1900i).

2.10 Kinetics Analysis

The oxidation of TMB with H_2O_2 by peptide-hemin complexes (steady-state kinetics) was measured by adding different amounts of TMB and H_2O_2 into the PBS buffer (pH 7.4 and 10 mM) containing each peptide-hemin complexes and the

absorbance at 640 nm was monitored by using a UV-vis spectrophotometer (UV-1900i) at 25 ℃. Final concentrations of reagents were: 10 μM of hemin and 100 μM of peptide, 0 - 8 mM of H_2O_2 and 0 - 0.8 mM of TMB. Initial rates of the reaction (v_0 was determined as the slope value for the linear part of the absorbance versus time plot within the first 20 s) were fitted to Michaelis-Menten kinetic mode.

3. Synthesis and characterizations of peptides

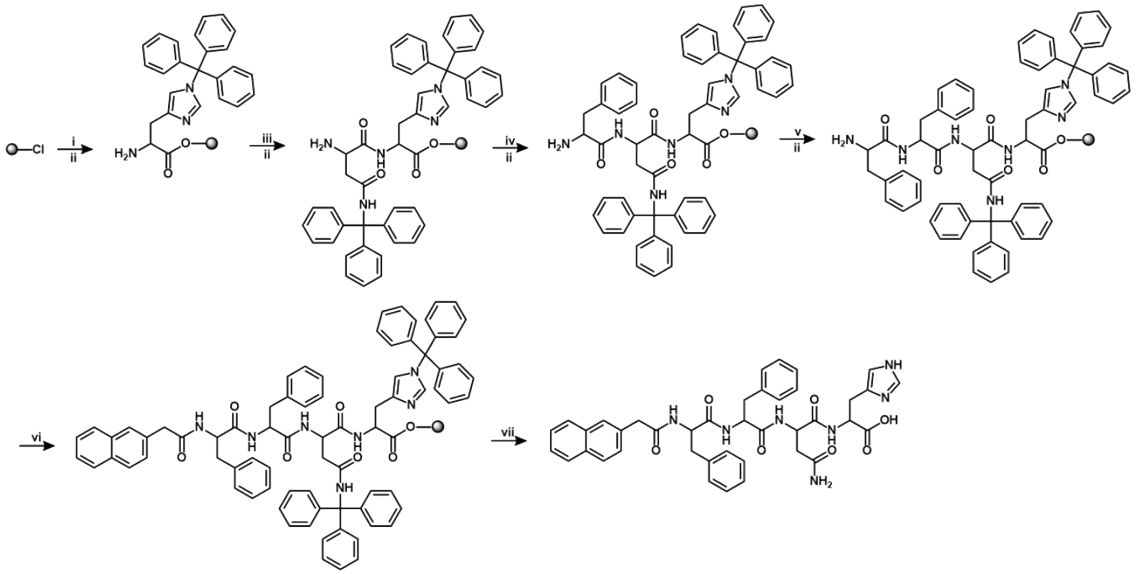

i)Fmoc-His(Trt)-OH,DIEA);ii) 20 % piperidine, DMF; iii)Fmoc-Asn(Trt)-OH, HBTU,DIEA; iv) Fmoc-Phe-OH, HBTU, DIEA; v) Fmoc-Phe-OH, HBTU, DIEA; vi) 2-Naphthylacetic acid, HBTU, DIEA; vii) TFA : H_2O =95 :5

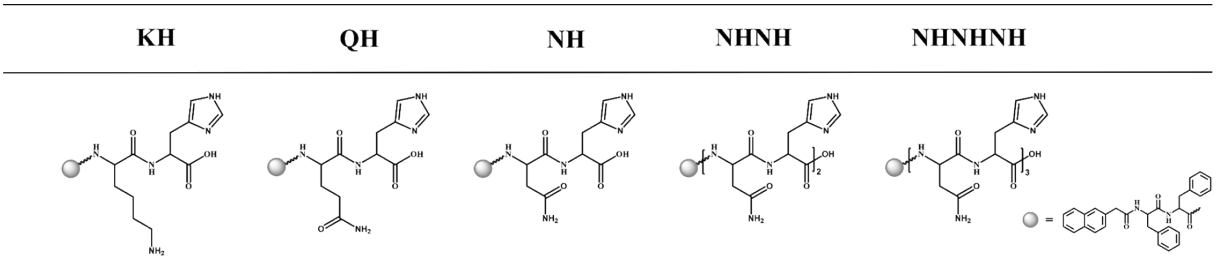

Fig. S1 Synthetic routes for the preparation of histidine-containing peptide

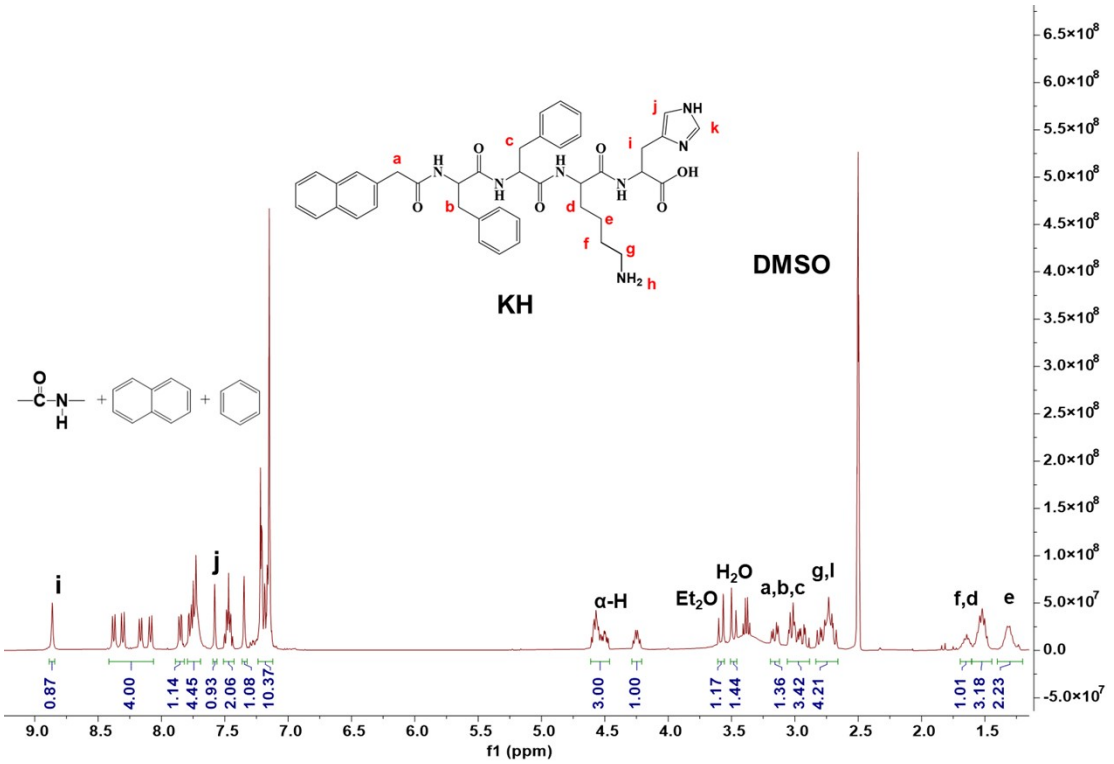

Fig. S2 ^{1}H NMR of KH in DMSO-*d6*

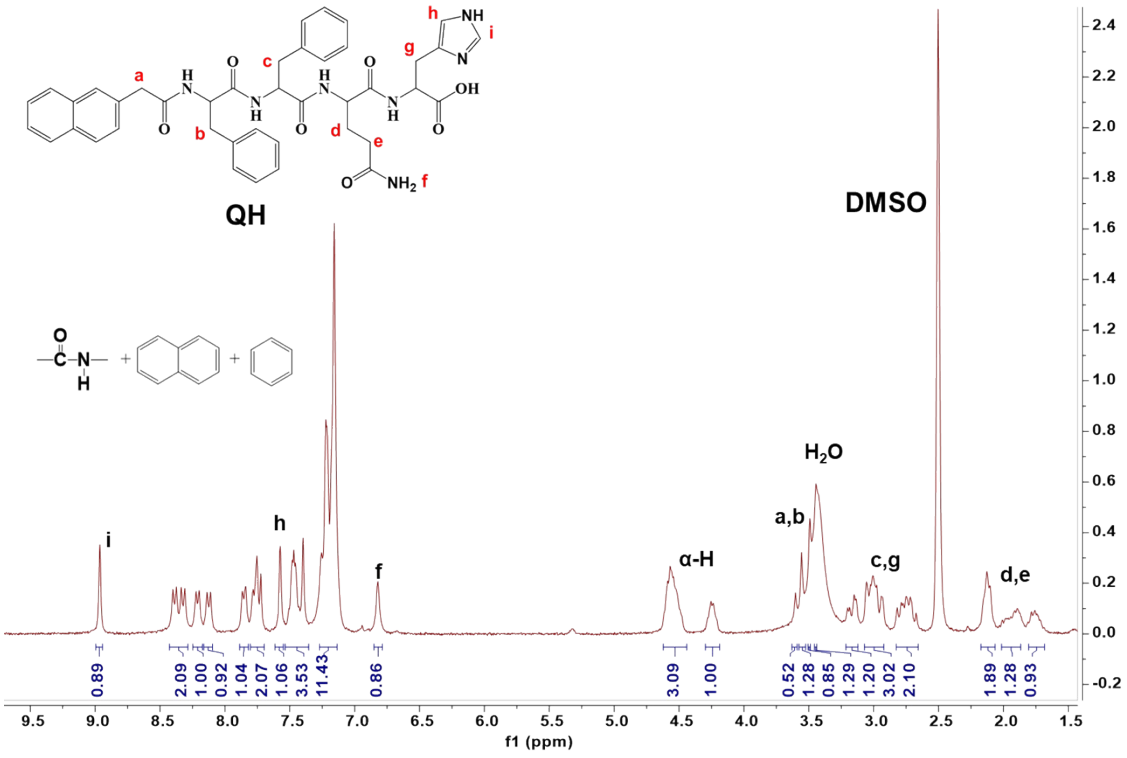

Fig. S3 ^{1}H NMR of QH in DMSO-*d6*

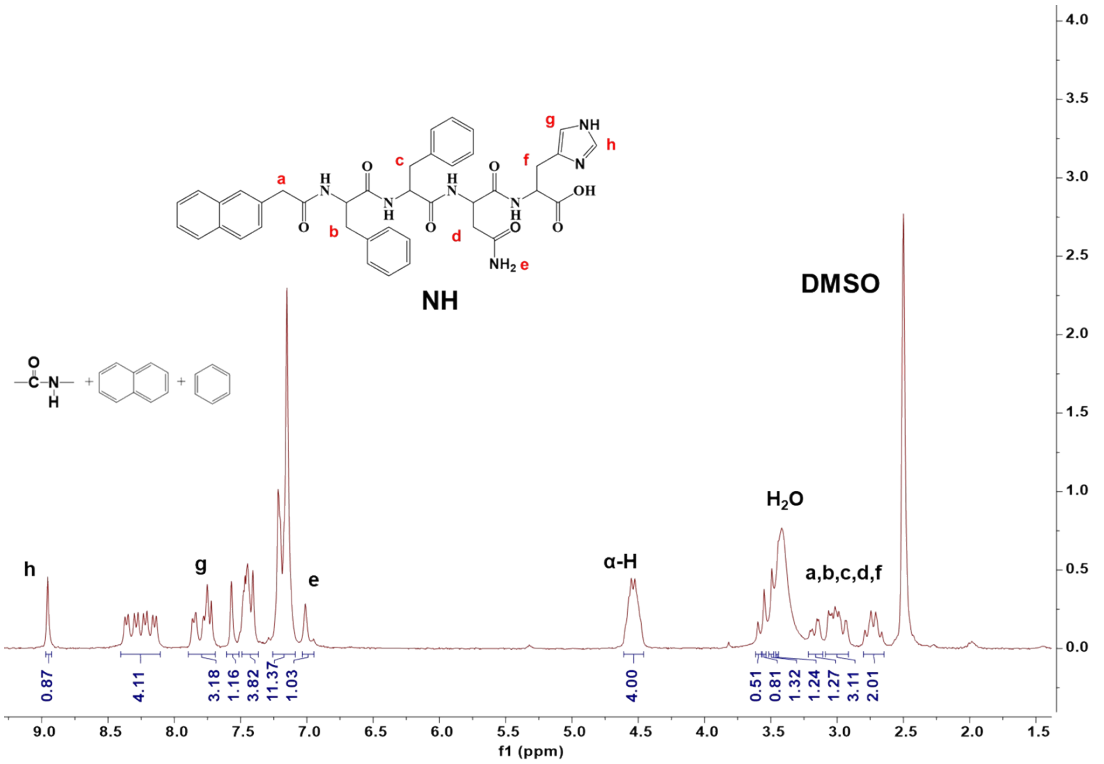

Fig. S4 ^{1}H NMR of NH in DMSO-*d6*

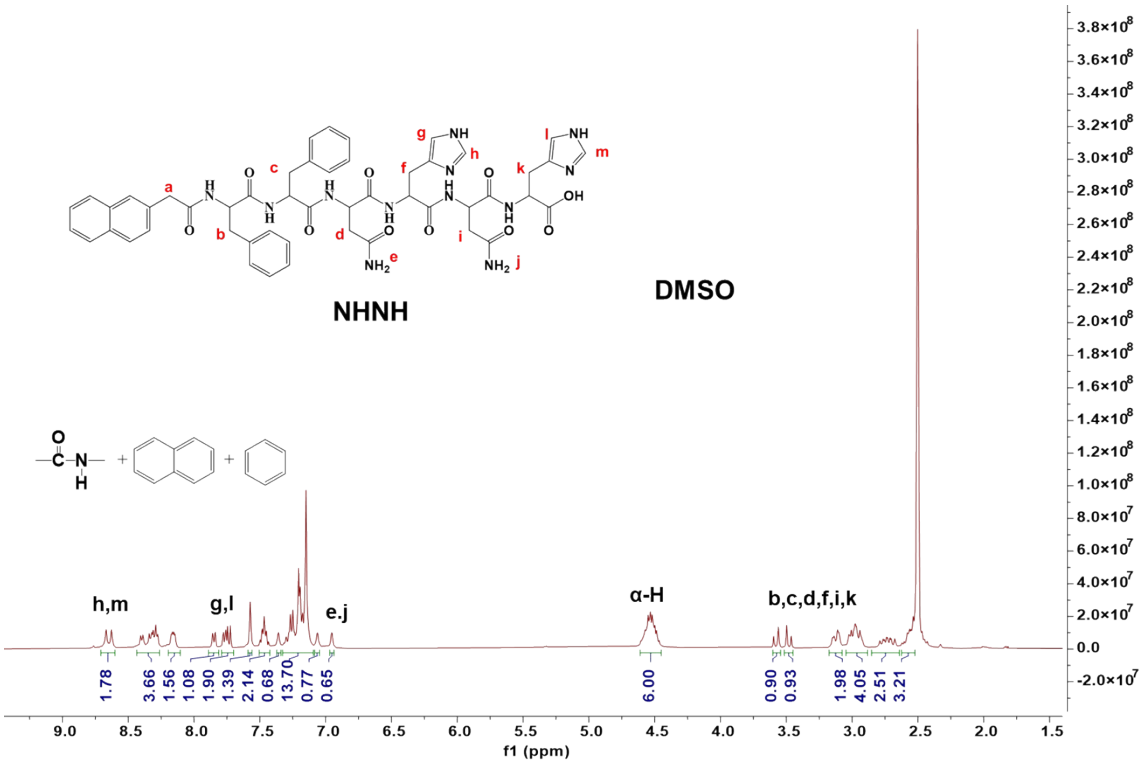

Fig. S5 ^{1}H NMR of NHNH in DMSO-*d6*

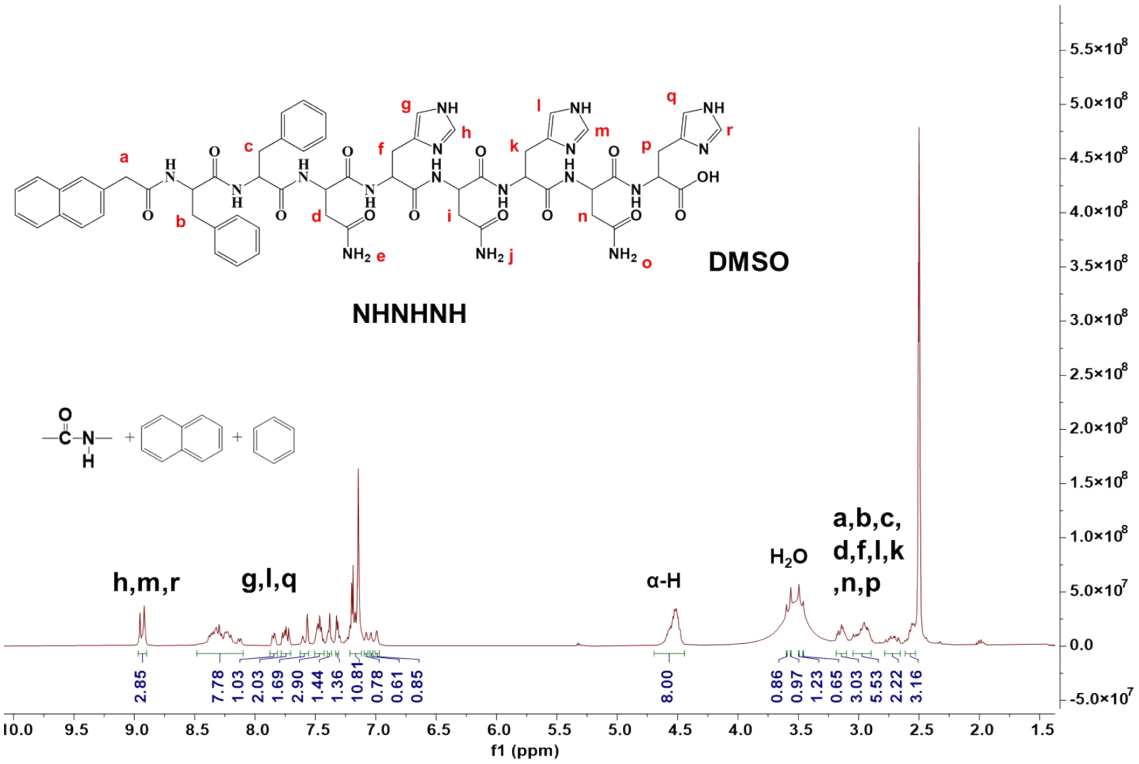

Fig. S6 ^{1}H NMR of NHNHNH in DMSO-*d6*

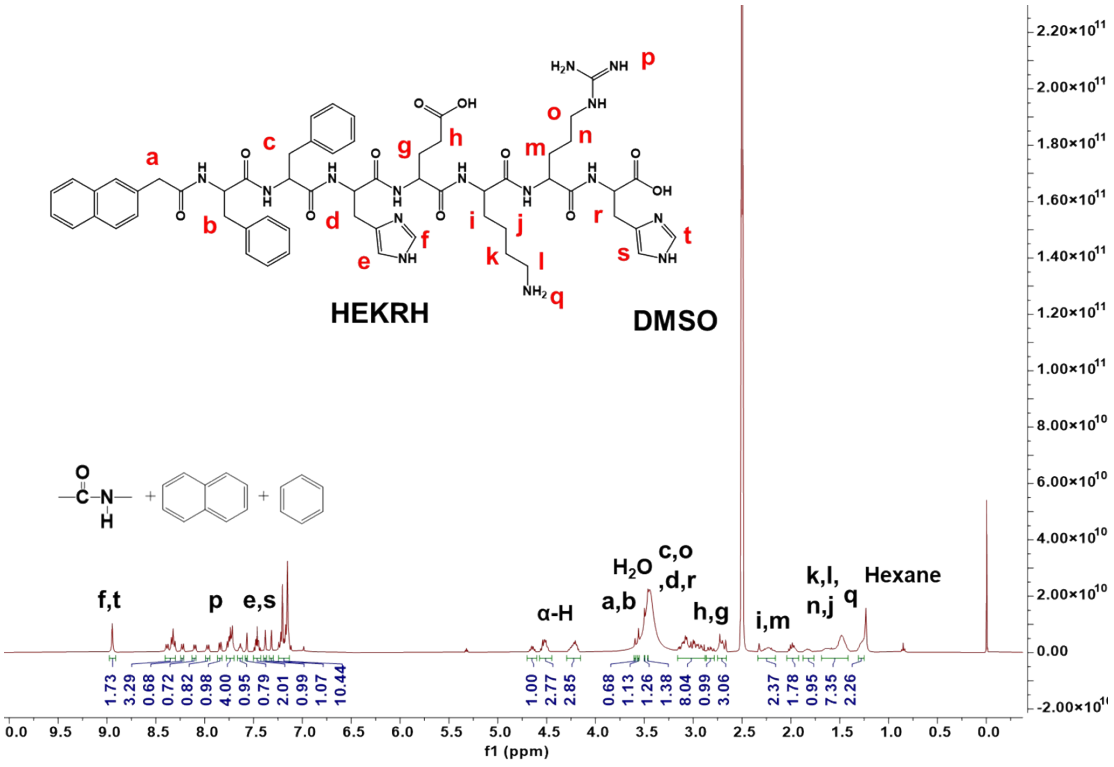

Fig. S7 ^{1}H NMR of HEKRH in DMSO-*d6*

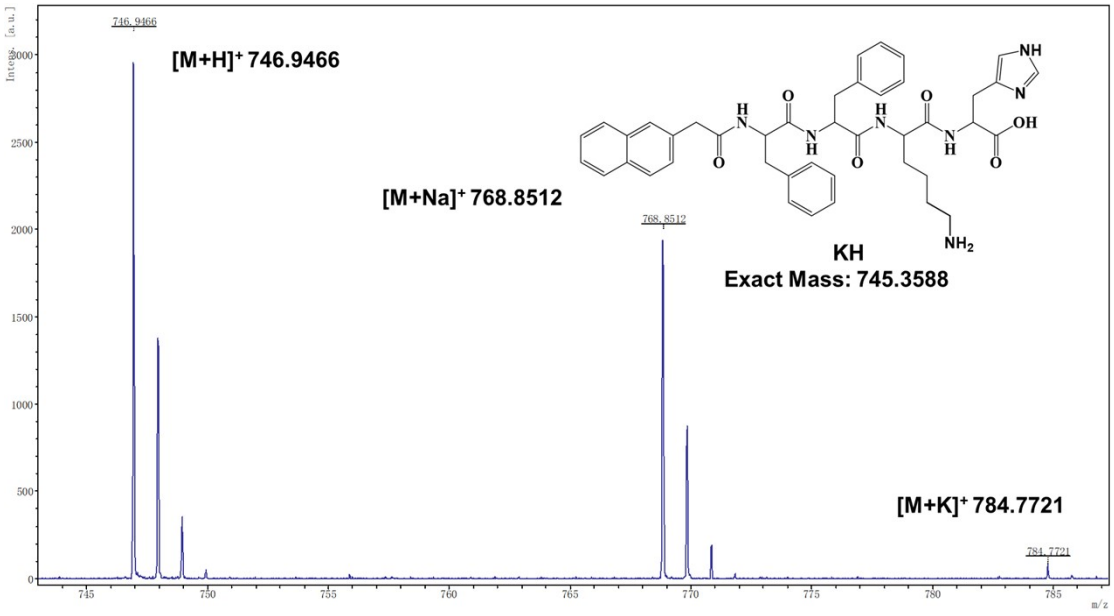

Fig. S8 MALDI-TOF mass spectrum of KH.

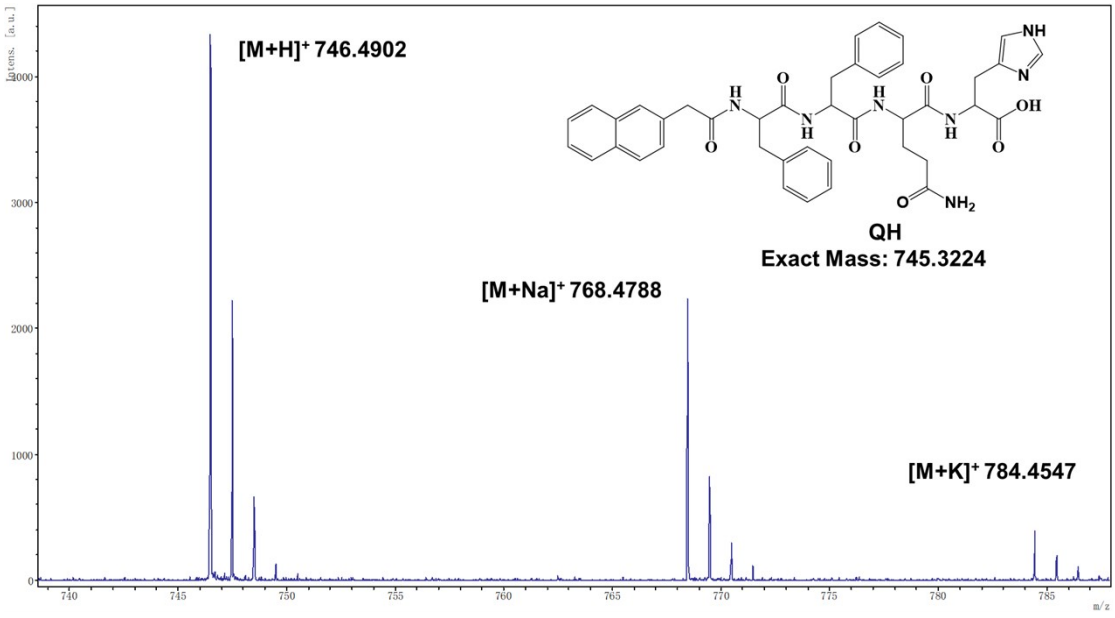

Fig. S9 MALDI-TOF mass spectrum of QH.

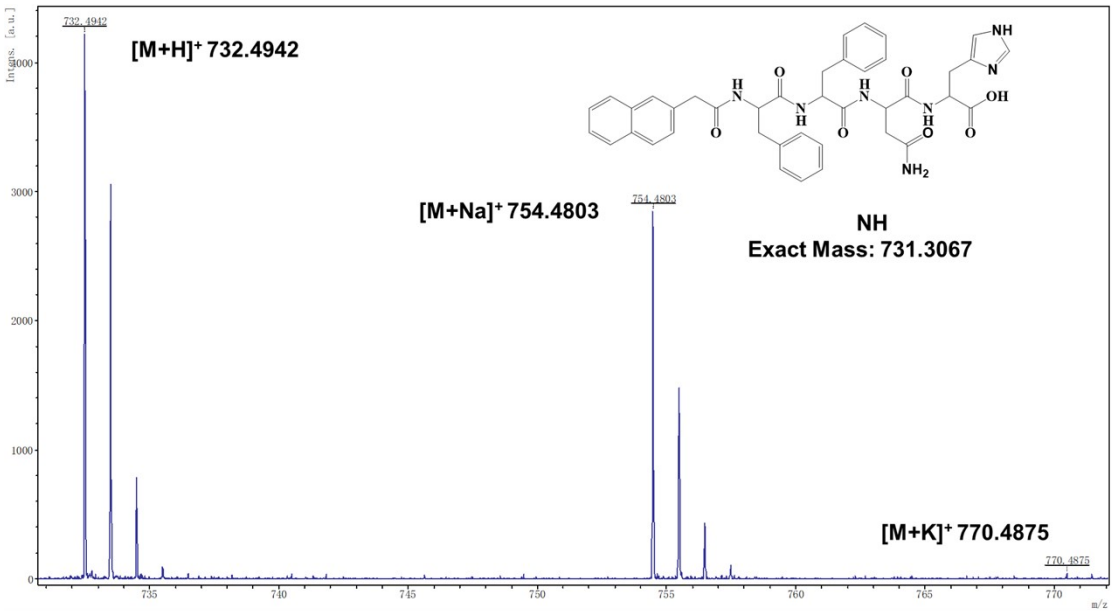

Fig. S10 MALDI-TOF mass spectrum of NH.

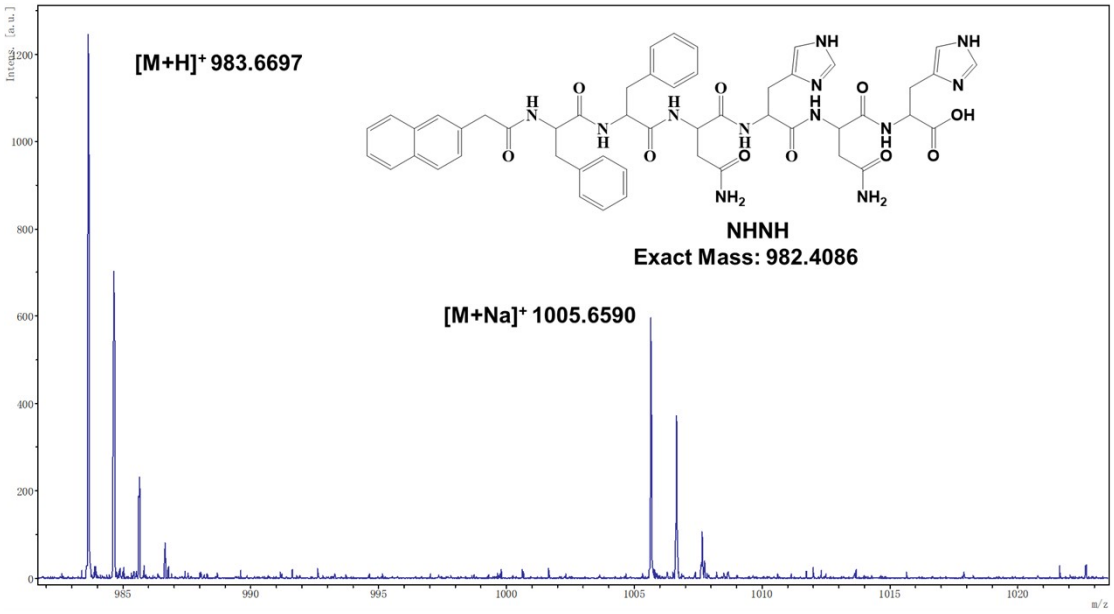

Fig. S11 MALDI-TOF mass spectrum of NHNH.

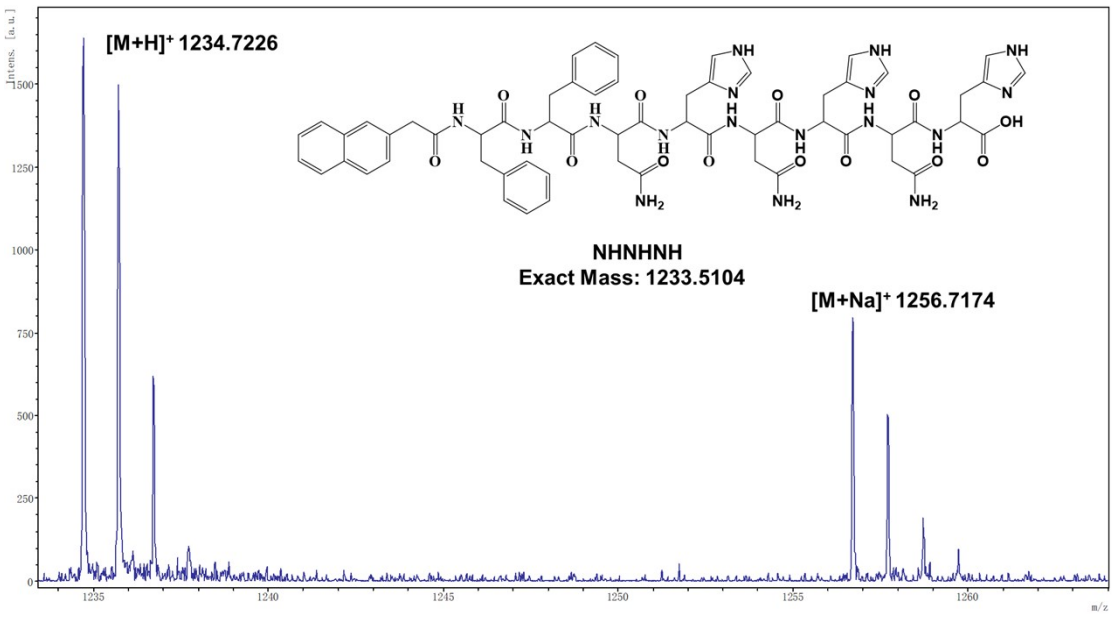

Fig. S12 MALDI-TOF mass spectrum of NHNHNH.

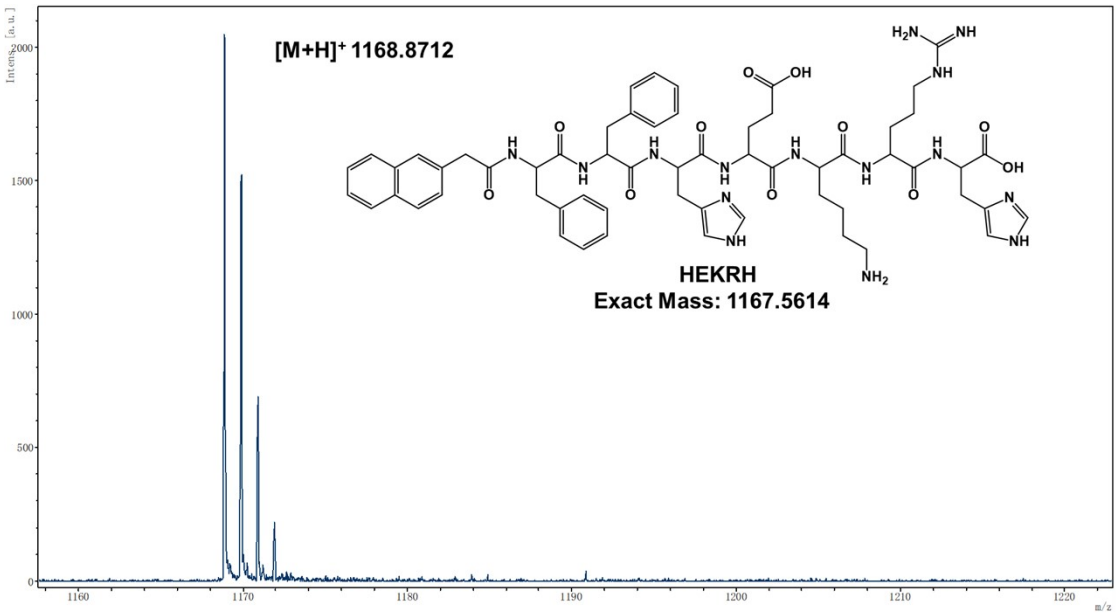

Fig. S13 MALDI-TOF mass spectrum of HEKRH.

4. Determination of the critical self-assembling concentration of peptides

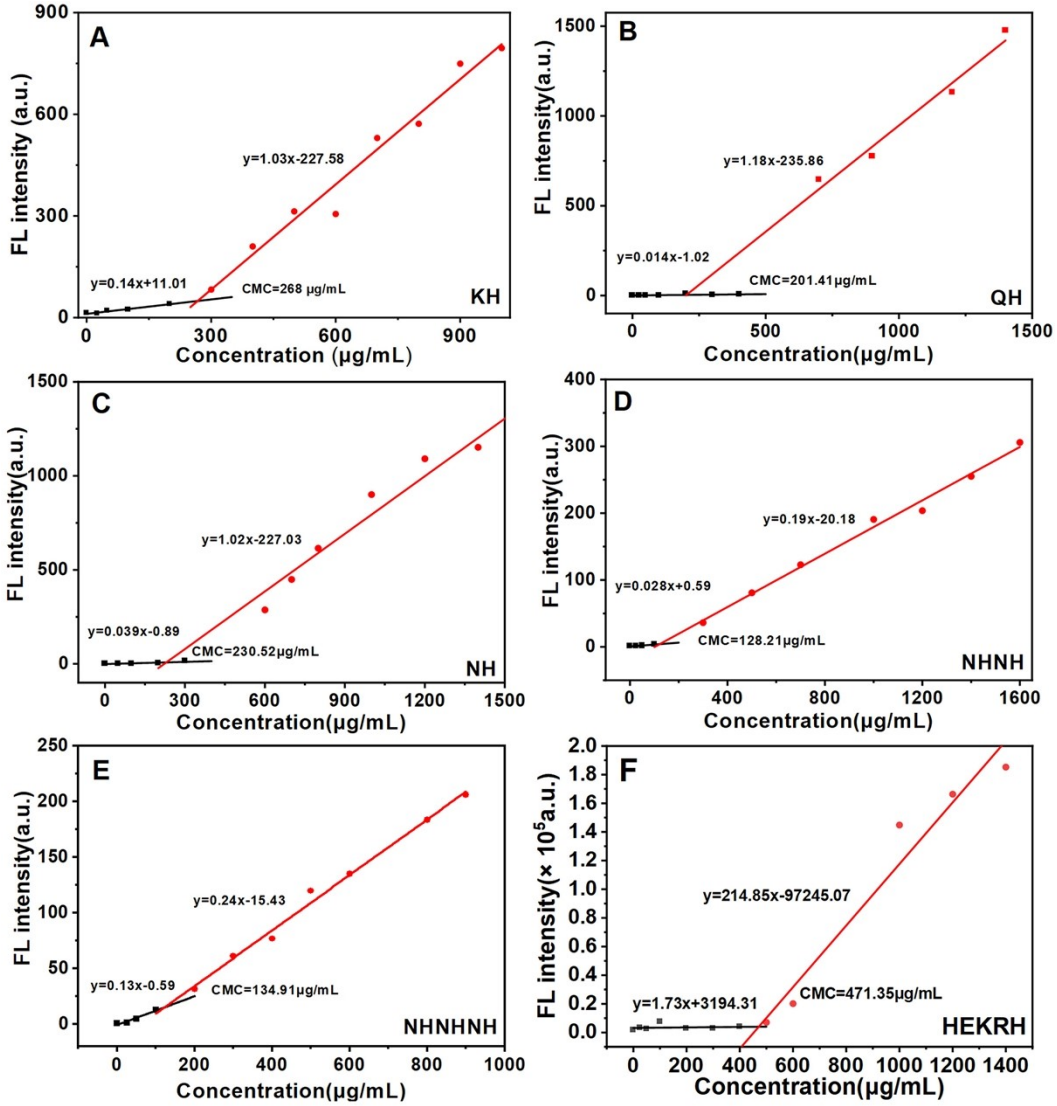

Fig. S14 The dose-dependent curves plotted with fluorescence intensities of Thioflavin T (2.0×10^{-5} M) versus varied concentrations of peptides.

5. Rheological measurements of peptide and peptide-hemin hydrogels

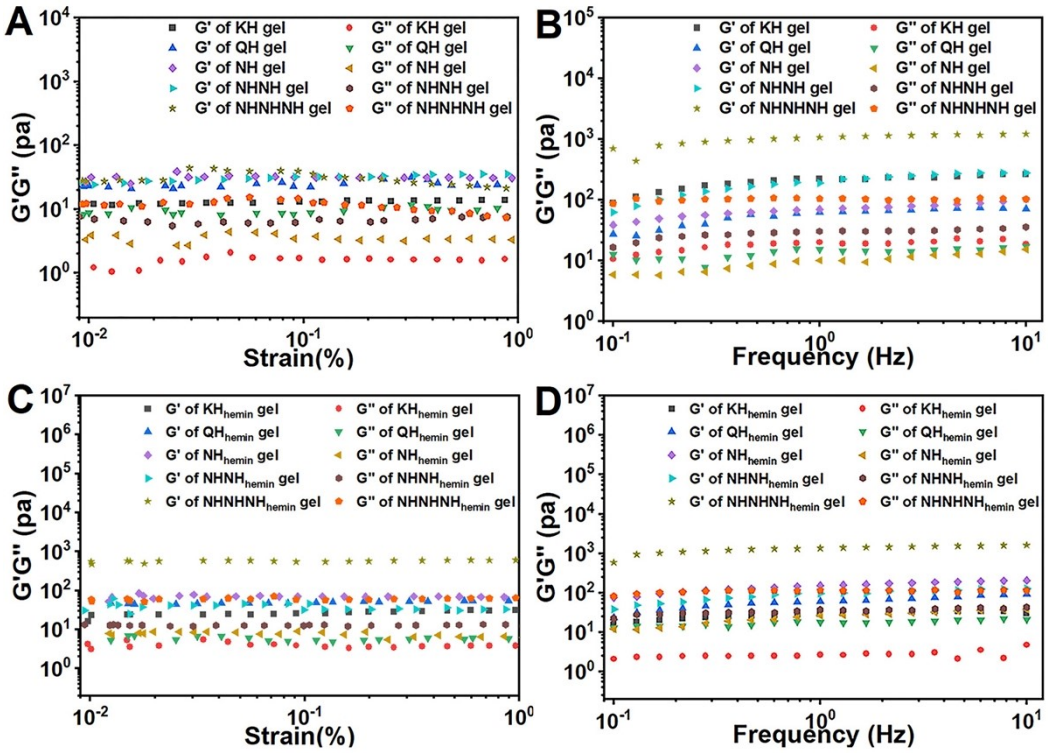

Fig. S15 (A) Strain and (B) frequency dependence of the dynamic storage moduli (G') and the loss moduli (G'') of peptide gels; (C) Strain and (D) frequency dependence of the dynamic storage moduli (G') and the loss moduli (G'') of peptide-hemin gels.

6. Gelation tests of the peptide-hemin complexes

Fig. S16 Optical images of the peptide-hemin (molar ratio 10:1) hydrogels from KH_{hemin} (0.1 wt%, pH 7.4), QH_{hemin} (3.0 wt%, pH 7.4), NH_{hemin} (0.5 wt%, pH 7.4), $NHNH_{hemin}$ (0.8 wt%, pH 7.4), and $NHNHNH_{hemin}$ (0.8 wt%, pH 7.4), respectively.

7. Peroxidase-like catalytic activities of peptide-hemin complexes

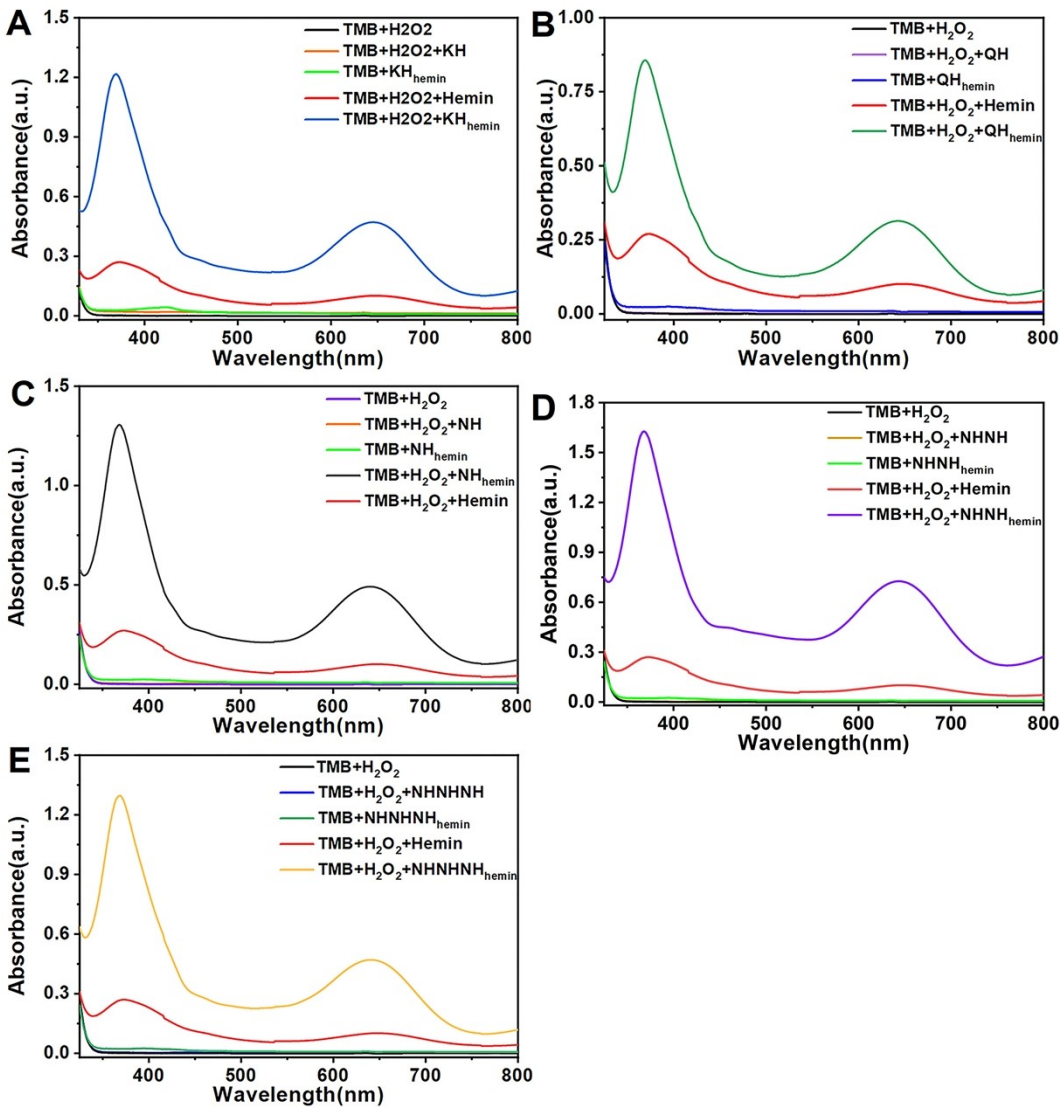

Fig. S17 Typical absorption spectra of TMB-H_2O_2 mixed solutions in different compositions.

8. Steady state kinetic analysis of peroxidase-like activities of hemin and peptide-hemin complexes

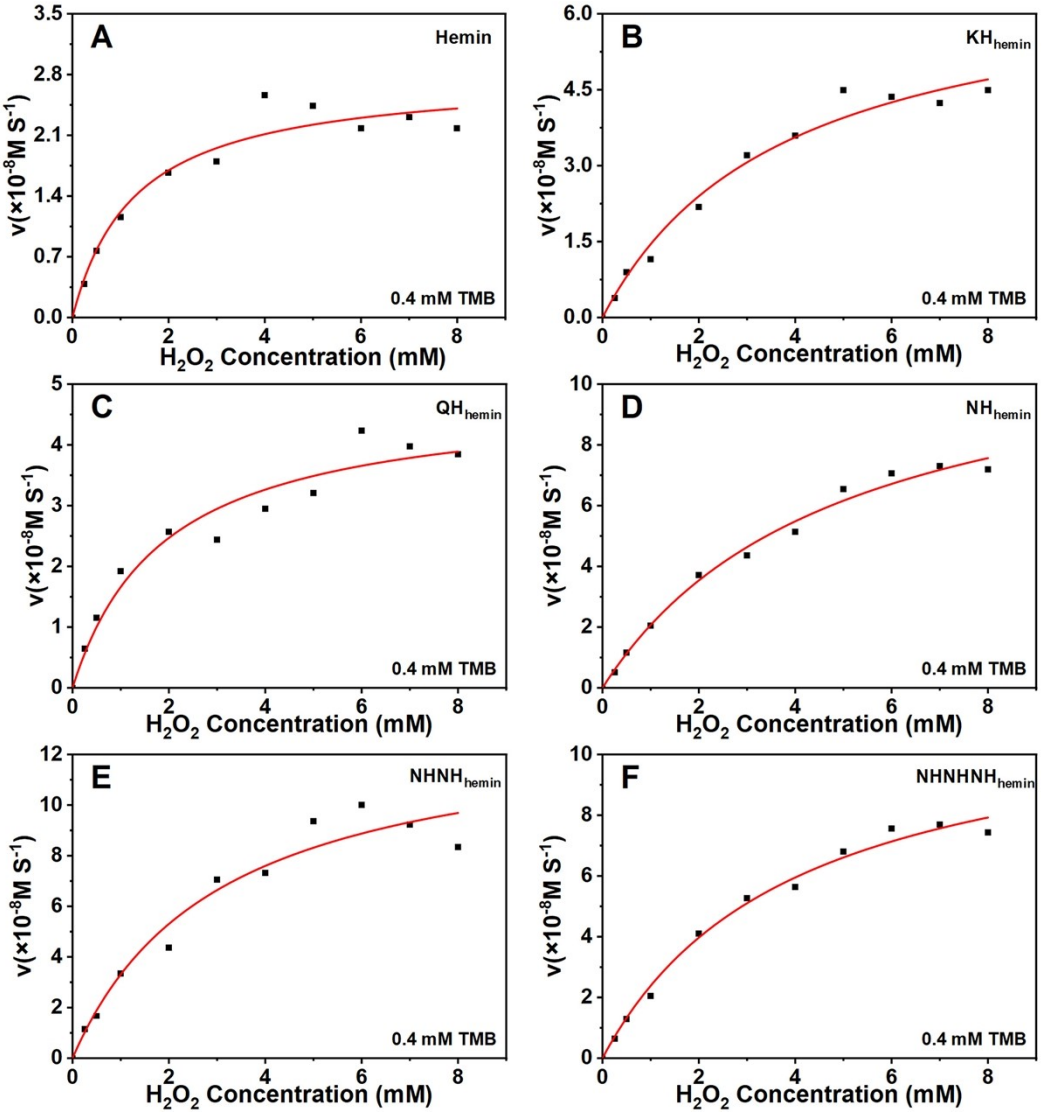

Fig. S18 (A-F) The Michaelis-Menten curves of peptide-hemin complexes for the oxidation of TMB by fixing the TMB concentration at 0.4 mM and varying H_2O_2 concentrations.

Table S1. Kinetic parameters of TMB oxidation by peptide-hemin complexes

Catalyst	V_{max} (×10^{-5} mM s^{-1})	k_{cat} (H_2O_2) (s^{-1})	K_M (H_2O_2) (mM)	k_{cat} / K_M (H_2O_2) (mM^{-1} s^{-1})
Hemin	2.80	0.028	1.30	0.022
KH$_{hemin}$	6.93	0.069	3.78	0.018
QH$_{hemin}$	4.8	0.048	1.9	0.025
NH$_{hemin}$	12.19	0.12	4.89	0.025
NHNH$_{hemin}$	13.38	0.13	3.04	0.043
NHNHNH$_{hemin}$	10.32	0.10	3.45	0.029

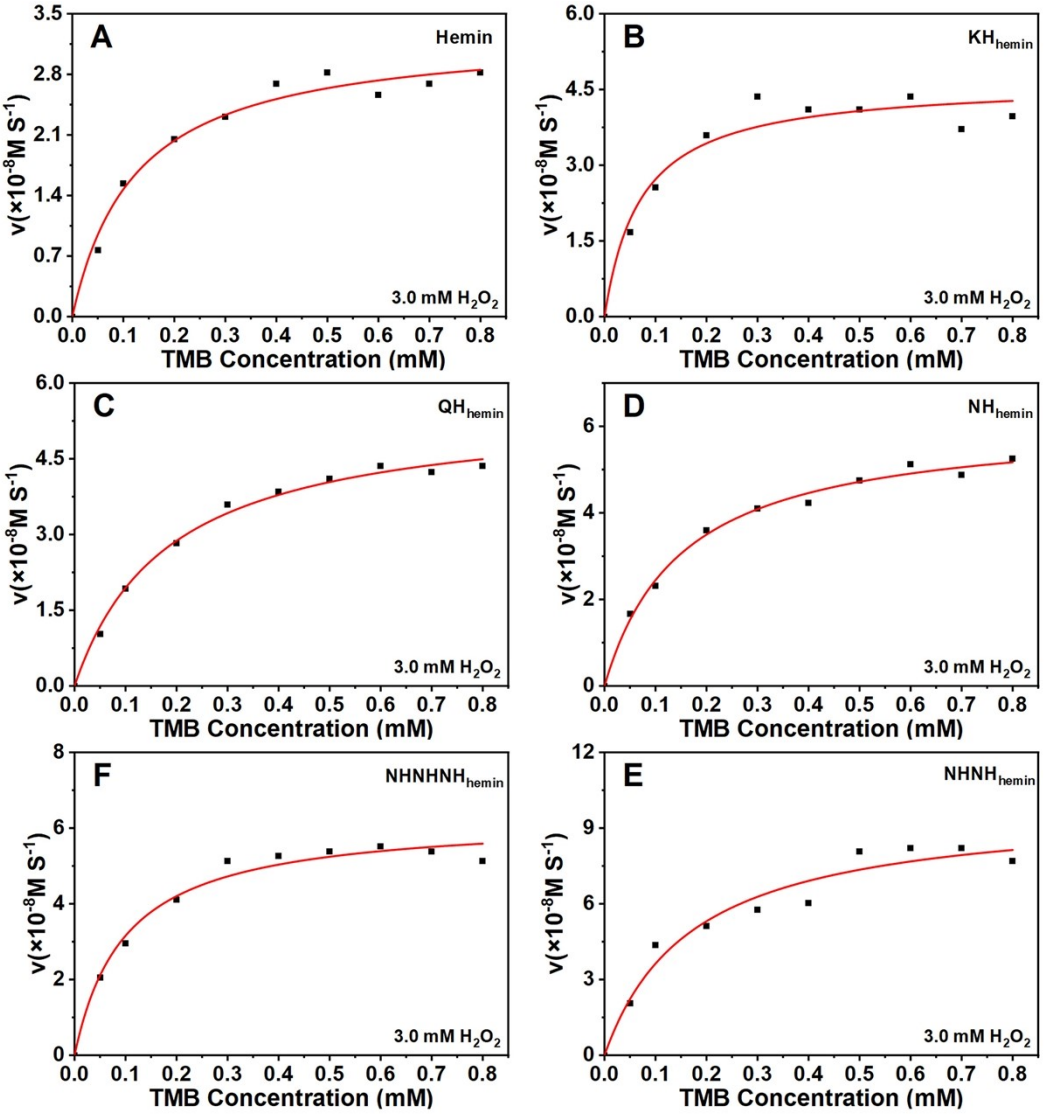

Fig. S19 (A-F) The Michaelis-Menten curves of peptide-hemin complexes for the oxidation of TMB by fixing the H_2O_2 concentration at 3 mM and varying TMB concentrations.

Table S2. Kinetic parameters of TMB oxidation by peptide-hemin complexes

Catalyst	V_{max} (×10^{-5} mM s^{-1})	k_{cat} (TMB) (s^{-1})	K_M (TMB) (mM)	k_{cat} / K_M (TMB) (mM^{-1} s^{-1})
Hemin	3.29	0.033	0.12	0.28
KH$_{hemin}$	4.65	0.047	0.071	0.66
QH$_{hemin}$	5.53	0.055	0.18	0.31
NH$_{hemin}$	6.15	0.062	0.15	0.41
NHNH$_{hemin}$	9.89	0.099	0.17	0.58
NHNHNH$_{hemin}$	6.28	0.063	0.099	0.63

9. Steady state kinetic analysis of peroxidase-like activities of NH_{hemin}, $HEKRH_{hemin}$, NH_{hemin}-HEKRH complexes

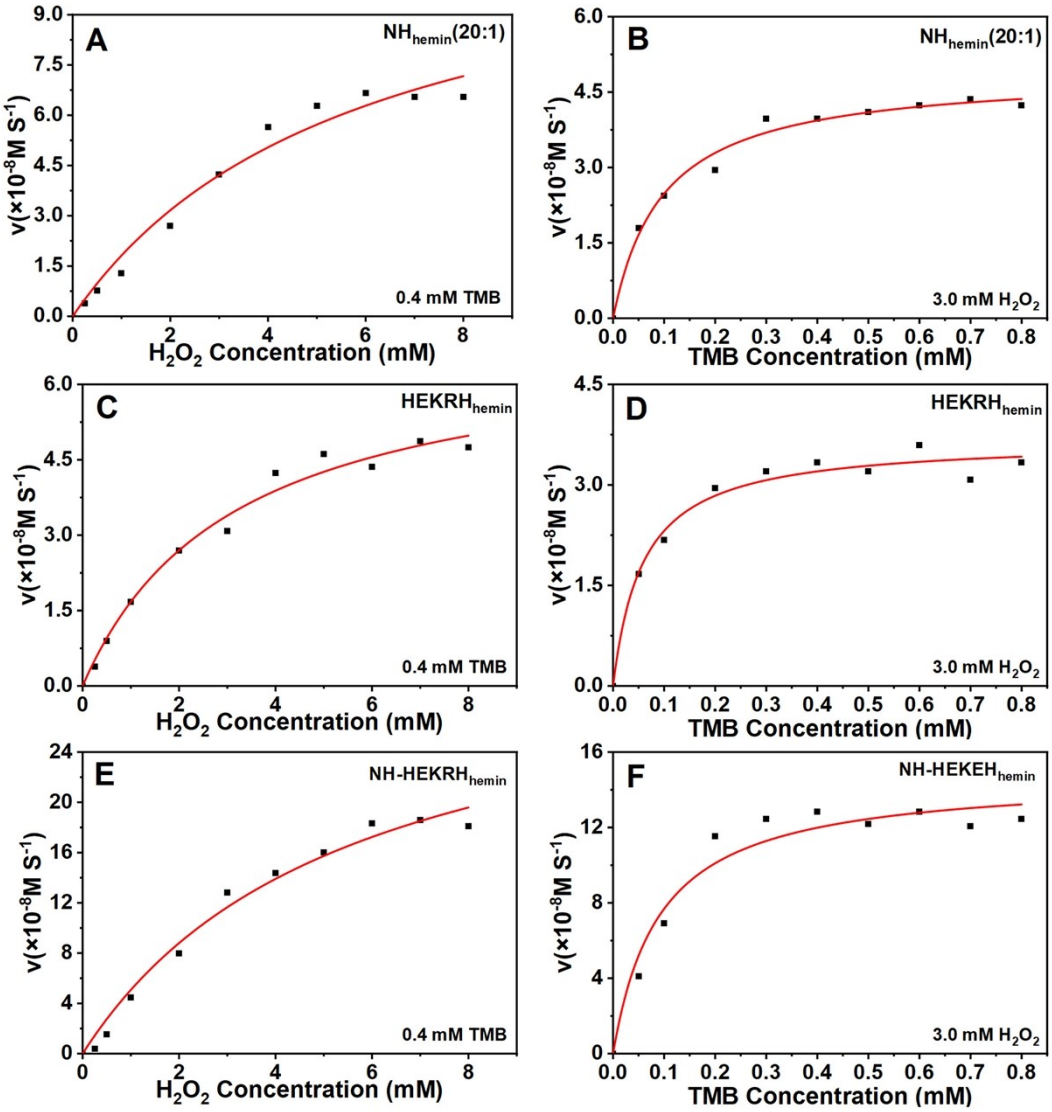

Fig. S20 The Michaelis-Menten curve of (A-B) NH_{hemin}, (C-D) $HEKRH_{hemin}$ and (E-F) NH-HEKRH-hemin complexes for the oxidation of TMB with the variation of TMB and H_2O_2 concentrations.

Table S3. Kinetic parameters of TMB oxidation by NH_{hemin}, $HEKRH_{hemin}$ and NH-HEKRH-hemin complexes

Catalyst	Substrate	V_{max} ($\times 10^{-8}$ M s^{-1})	K_M (mM)	k_{cat} (s^{-1})	k_{cat} / K_M (mM^{-1} s^{-1})
NH_{hemin} (20:1)	H_2O_2	12.39	5.83	0.12	0.021
NH_{hemin} (20:1)	TMB	4.89	0.10	0.049	0.49
$HEKRH_{hemin}$ (1:1)	H_2O_2	6.94	3.14	0.069	0.022
$HEKRH_{hemin}$ (1:1)	TMB	3.67	0.059	0.037	0.63
NH-HEKRH-hemin（20:1:1）	H_2O_2	33.12	5.53	0.33	0.060
NH-HEKRH-hemin（20:1:1）	TMB	12.89	0.069	0.13	1.88